JOURNAL OF MAGNETIC RESONANCE **134,** 214–222 (1998)
ARTICLE NO. MN981503

In Vivo 3D Localized ^{13}C Spectroscopy Using Modified INEPT and DEPT

H. Watanabe,*,[1] Y. Ishihara,* K. Okamoto,* K. Oshio,† T. Kanamatsu,† and Y. Tsukada†

**Toshiba Research and Development Center, Kawasaki 210-8582, Japan, and †Institute of Life Science, Soka University, Hachioji 192-8577, Japan*

Received December 22, 1997; revised April 21, 1998

The 3D localized ^{13}C spectroscopy methods LINEPT and LODEPT, which are modifications of INEPT and DEPT, are proposed. As long as a ^{13}C inversion pulse (180-degree pulse) is applied at 1/(4*J*) before the proton echo time in LINEPT and a ^{13}C excitation pulse (90-degree pulse) is applied at 1/(2*J*) before the proton echo time in LODEPT, the proton echo time can be set to any value longer than 1/(2*J*) in LINEPT and longer than 1/*J* in LODEPT. As a result, the proton and the ^{13}C pulses can be applied separately and these proton pulses can be made slice-selective pulses. These localization features of LINEPT and LODEPT were evaluated using a phantom consisting of a cylinder filled with ethanol placed inside another cylinder filled with oil, and localized ethanol spectra could be obtained. *In vivo* **3D localized ^{13}C spectra from the brain of a monkey could be obtained using decoupled LINEPT, and glutamate C-4 appeared directly after the administration of glucose C-1, followed by the appearance of glutamate C-2, C-3 and glutamine C-2, C-3, C-4.**

Key Words: **^{13}C-MRS**; *in vivo;* **localization; INEPT; DEPT.**

INTRODUCTION

^{13}C magnetic resonance spectroscopy (MRS) has been shown to be a powerful noninvasive technique for the study of metabolism. There are, however, problems associated with this technique, such as low sensitivity, and localization difficulty because of the large chemical-shift dispersion.

The nuclear Overhauser effect (NOE) has generally been used to overcome its low sensitivity. However, the enhancement factor by NOE is at most 3. This also gives rise to body heating caused by the high decoupling power.

Polarization transfer gives a better signal-to-noise ratio, since the enhancement factor is 4 and signal recovery is determined by the proton's short T_1. Polarization transfer will also give lower decoupling power, since decoupling is on only during the acquisition time. Moreover, the polarization transfer method will be a useful technique for localization because it can make use of localization on the proton. The advantages of using localization on the proton are, first, that the accuracy of localization improves because the proton chemical-shift dispersion is small and, second, that the required gradients are reduced by a factor of 4.

For these reasons, several techniques using polarization transfer have been developed (*1–4*), but some problems remain, such as complicated RF pulses (*1*), contamination due to T_1 recovery (*1, 2*), impossibility of 3D localization (*3, 4*), and signal loss because of the proton chemical shift effects on polarization transfer (*4*). In this paper, we propose two new three-dimensional localization techniques, LINEPT (localized INEPT (*5*) (insensitive nuclei enhanced by polarization transfer)) and LODEPT (localized DEPT (*6*) (distortionless enhancement by polarization transfer)), which can be applied on a whole-body scanner, and we present the results of phantom and animal experiments performed to verify the usefulness of these techniques.

THEORY

3D Localized ^{13}C Spectroscopy

In INEPT (Fig. 1a) and DEPT (Fig. 2a), the proton 180-degree pulses enable polarization transfer without proton chemical shift effects. Moreover, three proton pulses make three-dimensional localization possible. However, when the second proton pulse is made slice selective in each sequence on a whole-body scanner, a position error between metabolites occurs using this gradient system whose maximum amplitude is normally about 10 mT/m. This is because the first ^{13}C pulse is also obliged to be applied at the same time as the slice gradient pulse in spite of the large ^{13}C chemical shift dispersion. The dispersion between glucose and its metabolites in the case of [1-^{13}C]glucose administration is about 100 ppm and the position error is 2 cm when a 10-mT/m slice gradient pulse is used on a 2-T MRI scanner. Since these proton and ^{13}C pulses can be applied separately in LINEPT and LODEPT (Figs. 1b, 2b) based on INEPT and DEPT, respectively (*7*), these methods can be applied on a whole-body scanner with a ^{13}C system.

First, we explain the case for LINEPT. In INEPT, the role of the proton 180-degree pulse is to refocus the proton chemical shifts and the role of the ^{13}C 180-degree pulse is to invert the ^{13}C spins. The essence of INEPT, therefore, is that the ^{13}C inversion pulse is applied at 1/(4*J*) before the proton echo time

[1] To whom correspondence should be addressed. Fax: 044-520-1308. E-mail: watanabe@eel.rdc.toshiba.co.jp.

1090-7807/98 $25.00

and the third proton pulse or at $1/(4J)$ after the first proton pulse. In the LINEPT sequence, as long as the time interval between the ^{13}C inversion pulse and the proton echo time or between the first proton pulse and ^{13}C inversion pulse is set to $1/(4J)$, INEPT-type polarization transfers with proton chemical shifts refocused can be created even in the proton echo time that is longer than $1/(2J)$. As a result, the proton refocusing pulse and the ^{13}C inversion pulse can be applied separately. Therefore, three proton pulses can be made slice-selective pulses in a whole-body scanner. Figure 1b shows the LINEPT sequence where a ^{13}C inversion pulse is applied at Δ_a equal to $1/(4J)$ before the proton echo time and the third proton pulse. Neglecting gradient pulses and proton chemical shifts for the sequence shown in Fig. 1b, the J evolution can be expressed as

$$I_z \xrightarrow{90^\circ_x(^1\mathrm{H})} \xrightarrow{\tau} \xrightarrow{180^\circ(^1\mathrm{H})} \xrightarrow{\tau - \frac{1}{4J}}$$

$$\frac{1}{\sqrt{2}} I_y + \frac{1}{\sqrt{2}} 2I_xS_z \text{ at } t_1$$

$$\xrightarrow{180^\circ(^{13}\mathrm{C})} \frac{1}{\sqrt{2}} I_y - \frac{1}{\sqrt{2}} 2I_xS_z \text{ at } t_2$$

$$\xrightarrow{\frac{1}{4J}} -2I_xS_z \quad \text{at } t_3$$

$$\xrightarrow{90^\circ_y(^1\mathrm{H})} 2I_zS_z \quad \text{at } t_4. \qquad [1]$$

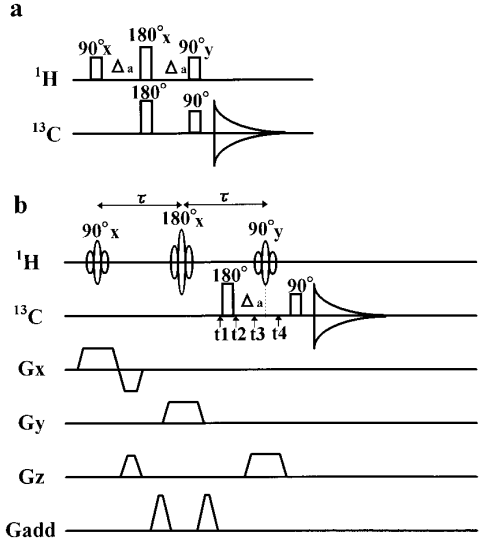

FIG. 1. Conventional INEPT sequence (a) and proposed LINEPT sequence (b). Δ_a is $1/(4J)$. As long as ^{13}C inversion pulse is applied at $1/(4J)$ before the proton echo time or at $1/(4J)$ after the first proton pulse, these proton and ^{13}C pulses can be applied separately. Polarization transfer from proton to ^{13}C occurs only inside a 3D localized volume, making three proton pulses slice selective pulses. The additional gradient pulses (Gadd) are applied for coherence clean selection. Conventional INEPT phase-cycling is shown here.

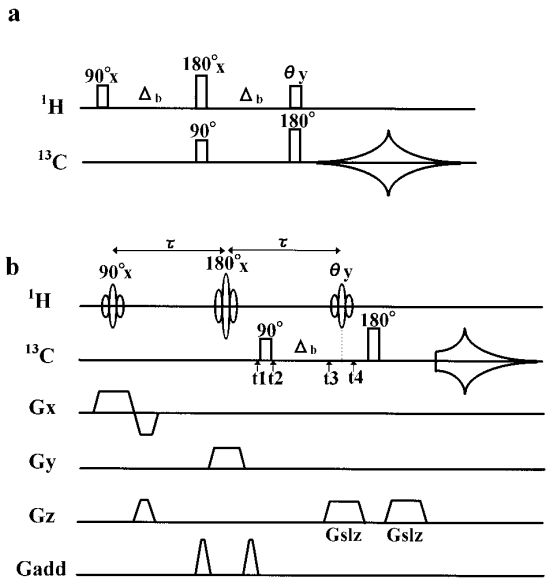

FIG. 2. Conventional DEPT sequence (a) and proposed LODEPT sequence (b). Δ_b is $1/(2J)$. Conventional DEPT phase cycling is shown here.

Thus, using three selective pulses, a $2I_zS_z$ of CH_n is created only inside a 3D localized volume and polarization transfer to ^{13}C occurs with the subsequent ^{13}C excitation pulse. Phase cycling is carried out to eliminate unenhanced ^{13}C signals which come from only ^{13}C pulses. The scheme is as follows: the third proton pulse phase $(y, -y)$ and the receiver phase $(x, -x)$. Additional gradient pulses are applied to eliminate unwanted echoes caused by imperfection of the proton refocusing pulse.

Similarly, ^{13}C polarization transfer signals can also be obtained only in a 3D localized volume using LODEPT. In the LODEPT sequence, as long as the time interval between the first ^{13}C pulse and the proton echo time or between the first proton pulse and the first ^{13}C pulse is set to $1/(2J)$, DEPT-type polarization transfers with proton chemical shifts refocused can be created even when the proton echo time is longer than $1/J$. As a result, the proton refocusing pulse and the first ^{13}C pulse can be applied separately. Therefore, three proton pulses can be used as slice-selective pulses, and 3D localization is possible in a whole-body scanner. Figure 2b shows the LODEPT sequence where the first ^{13}C pulse is applied at Δ_b equal to $1/(2J)$ before the proton echo time and the third proton pulse. Neglecting gradient pulses and proton chemical shifts for the sequence shown in Fig. 2b, J evolution of CH_n can be expressed as

$$I_{kz} \xrightarrow{90^\circ_x(^1\mathrm{H})} \xrightarrow{\tau} \xrightarrow{180^\circ(^1\mathrm{H})} \xrightarrow{\tau - \frac{1}{2J}}$$

$$2I_{kx}S_z \quad \text{at } t_1$$

$$\xrightarrow{90^\circ_x(^{13}\mathrm{C})} -2I_{kz}S_y \quad \text{at } t_2$$

$$\xrightarrow{\frac{1}{2J}} -2I_{kx}S_y \ \mathrm{CH} \quad \text{at } t_3$$

$$4I_{kx}I_{k'z}S_x \ \mathrm{CH_2}$$

$$8I_{kx}I_{k'z}I_{k''z}S_y \ \mathrm{CH_3}. \qquad [2]$$

After the third proton pulse, the θ pulse, observable is as follows:

$$\xrightarrow{\theta_y(^1\mathrm{H})} 2I_{kz}S_y \sin\theta \ \mathrm{CH} \quad \text{at } t_4$$

$$-4I_{kz}I_{k'z}S_x \sin\theta\cos\theta \ \mathrm{CH_2}$$

$$-8I_{kz}I_{k'z}I_{k''z}S_y \sin\theta\cos^2\theta \ \mathrm{CH_3}. \qquad [3]$$

Since ^{13}C magnetization is transversal after the first ^{13}C 90-degree pulse, the third slice gradient pulse Gslz dephases these ^{13}C spins. Therefore, Gslz has to also be applied after the ^{13}C refocusing pulse to rephase these ^{13}C spins (Fig. 2b). The phase cycling scheme for eliminating unenhanced ^{13}C signals is similar to the LINEPT case: the third proton pulse phase $(y, -y)$ and the receiver phase $(x, -x)$.

EXPERIMENTAL

Phantom and animal experiments were performed using a 2-T whole-body MRI scanner for ^{13}C spectroscopy (Toshiba, Japan).

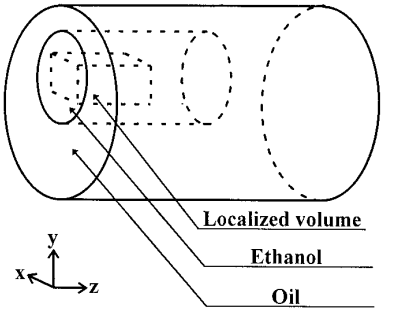

FIG. 3. Sketch of a phantom for localization evaluation of LINEPT and LODEPT. The 3D localized volumes were set inside the ethanol. The volume was 20 (x) × 20 (y) × 30 (z) mm^3.

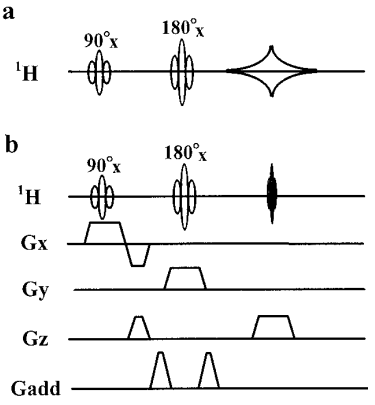

FIG. 4. RF phase adjustment sequences. B_0 shifts of proton spins bound to ^{13}C spins cause signal loss because the perpendicular relation between the phase of the proton spins and that of the third proton pulse in LINEPT and LODEPT is broken. The difference between the water proton signal phase using the SE sequence (a) and the phase using SE with localization and additional gradient pulses (b) was measured, to measure the phase difference.

Phantom Experiments

The RF coil consists of two perpendicular saddle coils, tuned to 85 MHz for protons (185 mm in diameter) and 21 MHz for ^{13}C (123 mm for ^{13}C). The phantom consists of a cylinder (37 mm in diameter, 70 mm in length) filled with ethanol placed inside another cylinder (65 mm in diameter, 90 mm in length) filled with baby oil (Johnson & Johnson, USA) (Fig. 3). The phantom was placed inside the RF coil and spectra were obtained by conventional INEPT and DEPT and by LINEPT and LODEPT. The phase cycling schemes explained in the theory section were used. The localized volume was inside the ethanol. In LINEPT and LODEPT, the proton TE was set to 20 ms and TR was 1 s. All the slice-selective pulses were $\pm 4\pi$ sinc pulses (4 ms in length) and all the ^{13}C pulses were rectangular pulses (200 μs in width). The time interval $1/(4J)$ was set to 1.8 ms for $J_{CH} = 140$ Hz and the flip angle of the third proton pulse in LODEPT was set to 45 degrees, both for optimal polarization transfer in ethanol C-1 (CH_2).

In LINEPT and LODEPT, using gradient pulses, B_0 shift occurs because of coupling between the gradient magnetic coils and the static magnetic coil. B_0 shift breaks the perpendicular relation between the phase of the third proton pulse and the signal phase of protons bound to ^{13}C spins at the proton echo time. As a result, the third proton pulse creates $2I_zS_z\cos(\Delta\theta)$, where $\Delta\theta$, is the phase difference, the polarization transfer signal losses. We overcame this problem by measuring $\Delta\theta$ caused by the B_0 shift to adjust the proton pulse phase. The scheme in the case of LINEPT was as follows. First, using a phantom filled with water, the water proton signal phase θ was obtained. A spin echo sequence consisting of the first LINEPT proton pulse and the second proton pulse was used (Fig. 4a). Next, the water proton signal phase θ_G was obtained using a pulse sequence consisting of the spin echo pulses and the LINEPT gradient pulses (Fig. 4b). The phase difference $(\theta_G - \theta)$ equals $\Delta\theta$. Therefore, the third proton pulse was applied

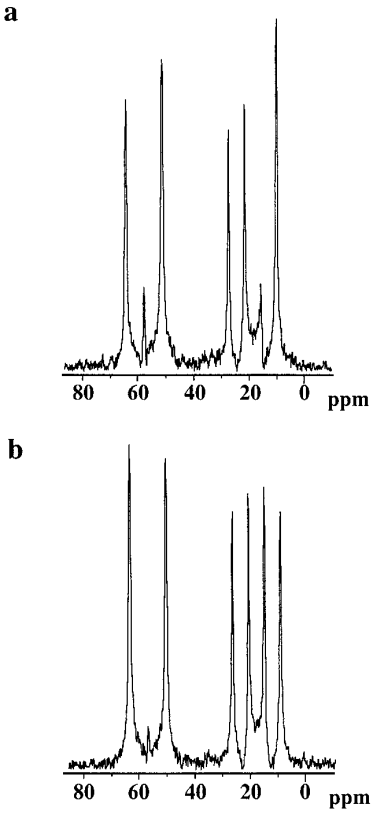

FIG. 5. Ethanol absolute spectra using a surface coil as the transmitter and receiver. The conventional INEPT sequence was used. Signal intensities between the peaks are not the same, and it is impossible to obtain the correct INEPT spectrum because of B_1 inhomogeneity using conventional two-phase cycling (a). The ratio of ethanol C-1 (CH_2) peaks is almost 1:1 and that of ethanol C-2 (CH_3) is almost 1:1:1:1 using our four-phase cycling (b). These features are all the same as those of INEPT.

at the phase ($\pi/2 + \Delta\theta$) in order to create the $2I_zS_z$ state and cause polarization transfer from proton to ^{13}C without loss. The adjustment method for the RF phase in LODEPT is the same as that described earlier. These adjustment procedures can be performed easily, since only two scans are needed to obtain the phase difference between water proton signals. Thus, the procedures can be performed again when the gradient conditions are changed or even when *in vivo* localized volume position is changed.

Inhomogeneity of RF amplitude may also cause signal loss, especially in the case of using a transmitter and receiver surface coil often used *in vivo*. Hence, phase cycling suitable for an inhomogeneous RF field needs to be designed. First, product operators were calculated for the case of arbitrary flip angle. Next, the phase cycling schemes were obtained to provide only the ^{13}C polarization transfer signals. In the case of INEPT, the obtained scheme shown as phase-cycling-1 in the Appendix was as follows: first proton pulse phase ($x, -x, x, -x$), first, ^{13}C pulse phase ($x, x, -x, -x$), and receiver phase ($x, -x, x, -x$). Figure 5 shows INEPT spectra of 99.5% ethanol obtained using a transmitter and receiver surface coil for proton and ^{13}C. The spectrum obtained by a conventional two-phase cycling scheme is compared with the spectrum obtained by this four-phase cycling scheme. In the two-phase cycling spectrum, methyl peaks are distorted, while in the four-phase cycling spectrum, these peaks have almost the same value.

Animal Experiments

Glutamate metabolism derived from D-[1-^{13}C]glucose in the brain of a monkey (*Macaca fascicularis*, female, 3.9 kg) was measured using decoupled and refocused LINEPT (Fig. 6), which consists of LINEPT pulses followed by a ^{13}C refocusing pulse and a proton decoupling pulse (WALTZ-4). There is another type of decoupled and refocused INEPT where the decoupling pulse is applied at a delay after a ^{13}C refocusing pulse with a proton inversion pulse; this type can also be applied to the decoupled and refocused LINEPT and can be used *in vivo*.

A double surface coil consisting of a ϕ 60-mm 4-turn ^{13}C surface coil and a figure-eight 60 × 100 mm proton coil was used. The localized volume (32 ml) was inside the brain. All the slice-selective pulses were $\pm 4\pi$ sinc pulses (4 ms in length). All the ^{13}C pulses were rectangular pulses (200 μs in width). The time intervals Δ_1 and Δ_2 (Fig. 6) in the decoupled and refocused LINEPT sequence were both set to 1.8 ms. The optimal delays will be considered in the Discussion section. Eight-phase cycling, designed using the same method as that in the phantom experiments, was as follows: first proton pulse phase $\phi 1$ ($x, -x, x, -x, x, -x, x, -x,$), first ^{13}C pulse phase $\phi 2$ ($x, x, -x, -x, x, x, -x, -x$), third carbon phase $\phi 3$ ($x, x, x, x, -x, -x, -x, -x,$), and receiver phase ($x, -x, x, -x, x, -x, x, -x$). The sampling time was 235 μs and the number of sampling points was 2048. Lorentz-to-Gaussian filtering (10 Hz) was used.

The surface coil was placed above the head of a monkey that had been anesthetized with ketamine (3.8 ml). A [1-^{13}C]ethanol reference phantom (ϕ 10 mm) was placed above the surface coil. The position of this reference phantom and that of the localized brain volume were almost symmetric with respect to the surface coil. RF power for proton and ^{13}C was tuned using the INEPT signal of the reference phantom. Shimming was done using the water proton FID signal.

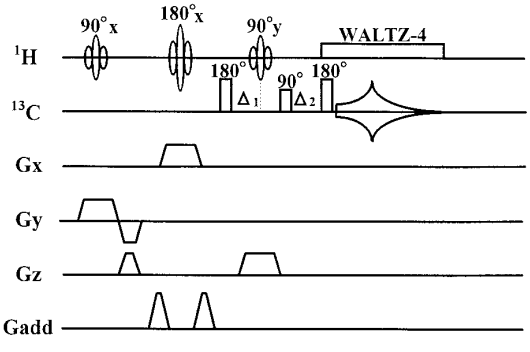

FIG. 6. Decoupled and refocused LINEPT sequence. Localized volume size is 40 (x) × 20 (y) × 40 (z) mm^3. The axis directions are shown in Fig. 8.

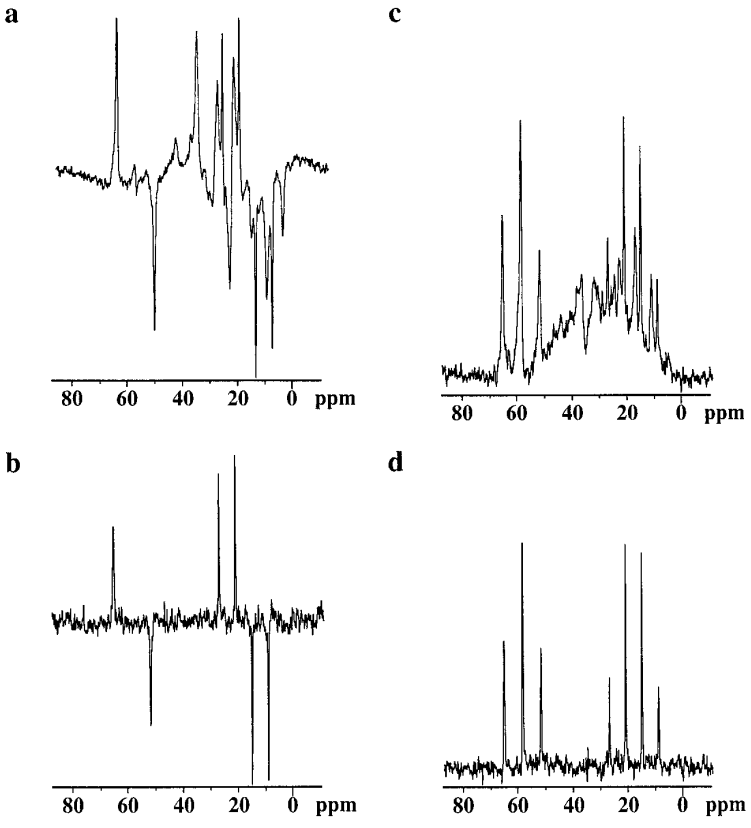

FIG. 7. Nonlocalized and localized phantom spectra. Contamination by oil signals is seen, in a conventional nonlocalized INEPT spectrum (a) and a DEPT spectrum (c). Only ethanol peaks are detected in a localized LINEPT spectrum (b) and a LODEPT spectrum (d).

Before glucose injection, nonlocalized spectra (a decoupled NOE enhanced spectrum and a decoupled INEPT spectrum) and a localized spectrum (a decoupled LINEPT spectrum) were obtained. TR was 1 s for each. Total acquisition time for NOE was 5 min, and 10 min each for INEPT and LINEPT.

The time course of decoupled LINEPT spectra was obtained

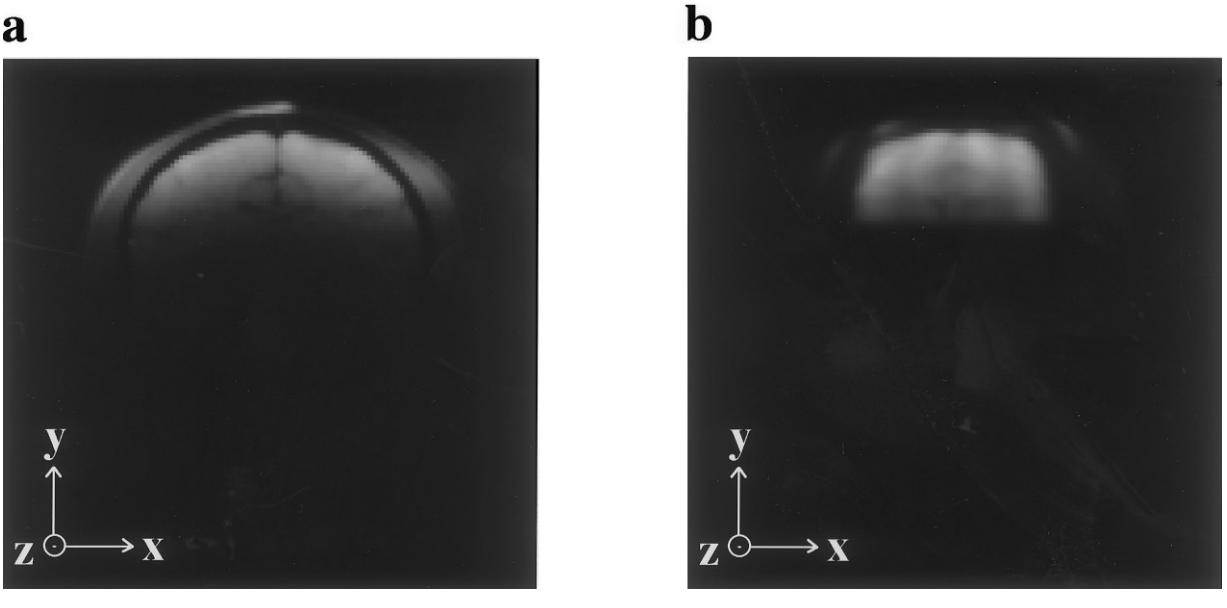

FIG. 8. ^{1}H coronal image of a monkey head (a) and localized coronal image (b).

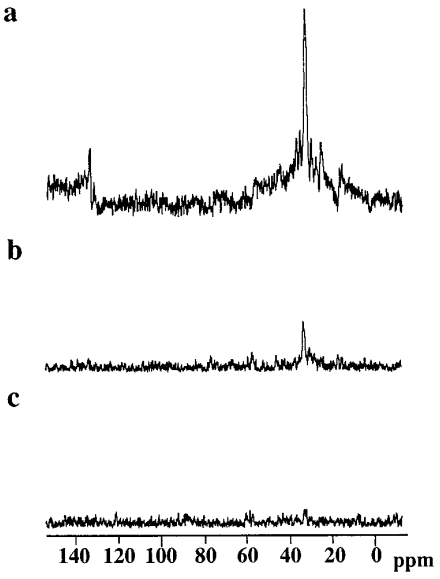

FIG. 9. Monkey head absolute spectra obtained using a ^{1}H decoupled ^{13}C-MRS sequence (a) and an INEPT sequence (b) and localized monkey brain absolute spectrum obtained using a decoupled LINEPT sequence (c). Contamination by lipid peaks is reduced in the decoupled LINEPT spectrum.

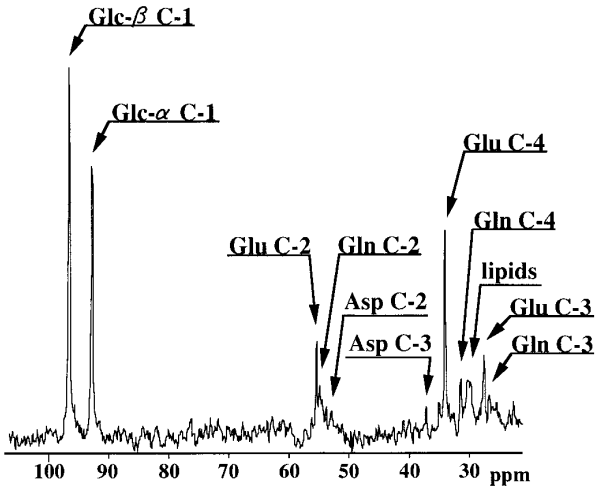

FIG. 10. *In vivo* decoupled 3D LINEPT spectrum acquired from monkey brain over 70 min. Each peak is clearly separated. In particular, glutamate C-2 and glutamine C-2, between which the chemical shift difference is only about 0.5 ppm, are clearly separated. Resonance assignments are as follows: Asp, aspartate; Glc, glucose; Gln, glutamine; Glu, glutamate.

after injecting D-[1-^{13}C]glucose (99% enriched, 1 g/kg body weight) intravenously into the monkey. TR was 1 s and total acquisition time was 10 min for each spectrum. Measurement was continued until 80 min after glucose injection.

RESULTS

Validation of Localization (Phantom Experiments)

In conventional INEPT and DEPT spectra, there is contamination by oil signals, while oil signals are eliminated in LINEPT and LODEPT spectra (Fig. 7). Features of the LINEPT spectrum are that the ratio of ethanol C-1 (CH_2) peaks is almost 1:−1 and that the ratio of ethanol C-2 (CH_3) peaks is almost 1:1:−1:−1. This is the same as the INEPT spectrum. The LODEPT spectrum has the features of a conventional ^{13}C spectrum in that the ratio of ethanol C-1 peaks is almost 1:2:1 and the ratio of ethanol C-2 peaks is almost 1:3:3:1. This is the same as the DEPT spectrum. Thus, we confirmed that 3D localized polarization transfer spectra could be obtained, using LINEPT and LODEPT.

Animal Experiments

A coronal image of the monkey head and a localized monkey brain image are shown in Fig. 8; the monkey head image is for the sensitive volume of nonlocalized NOE and INEPT spectra and the localized image is for the sensitive volume of LINEPT spectra. In the NOE spectrum before glucose injection, contamination by lipid peaks, arising from natural-abundance methylene (near 30 ppm) and olefinic (near 129 ppm) carbons is observed (Fig. 9a (*8*)). In the decoupled and refocused INEPT spectrum, the methylene ^{13}C peak height is decreased and the olefinic ^{13}C peak is absent, because of signal loss due to B_1 distribution of the surface coil (Fig. 9b). In the decoupled and refocused LINEPT spectrum from the monkey brain, these lipid peaks are further decreased (Fig. 9c). In the decoupled LINEPT spectrum after glucose injection, glucose and several amino acid peaks are detected, and glutamate C-2 and glutamine

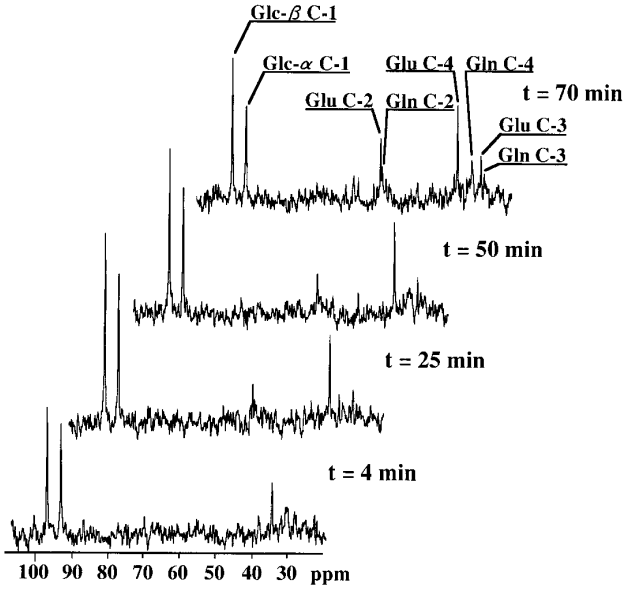

FIG. 11. Stacked plot of decoupled 3D LINEPT spectra obtained from monkey brain *in vivo.* Each spectrum was acquired over 10 min.

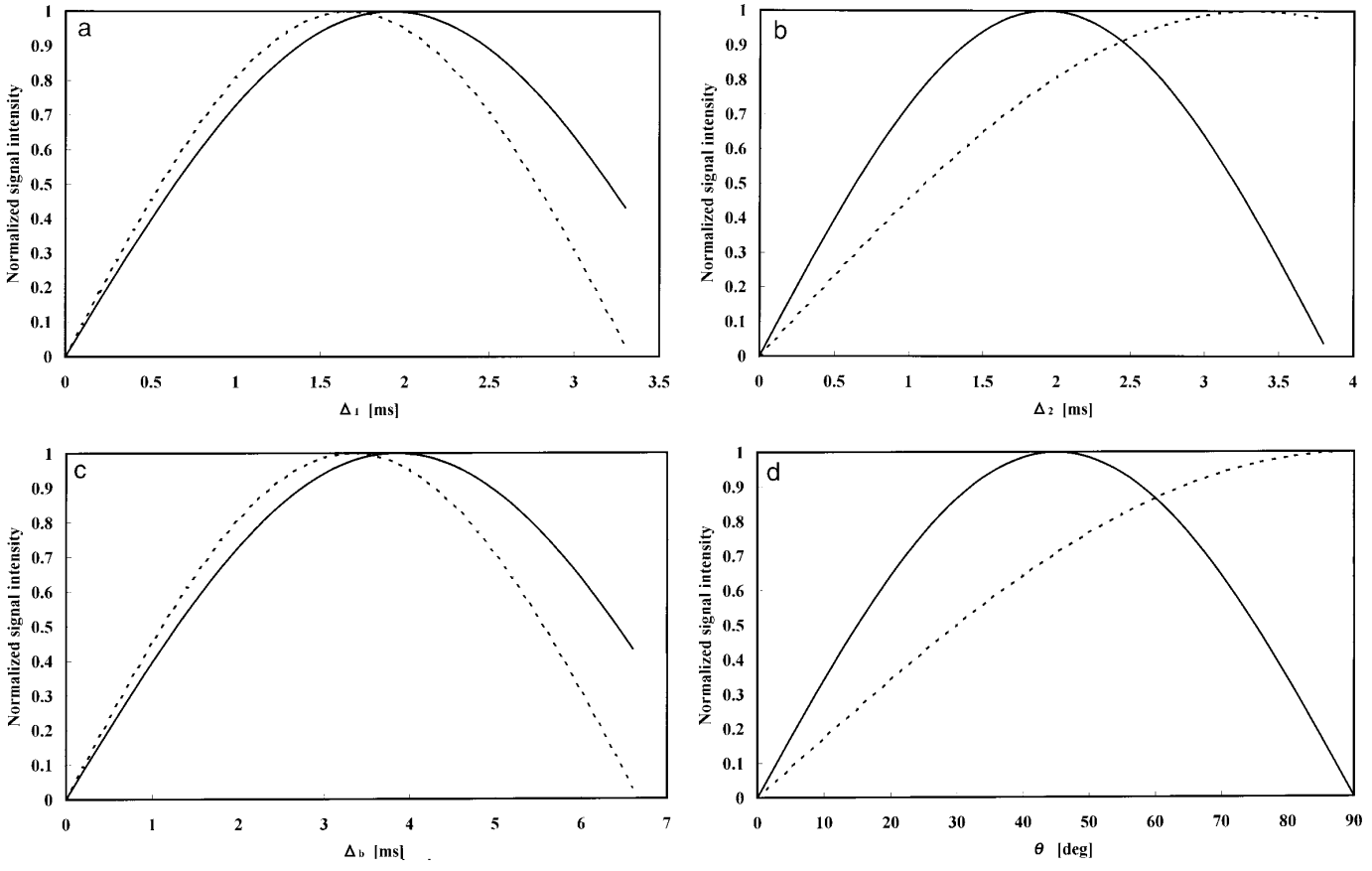

FIG. 12. Relationship between the signal intensities and Δ_1, Δ_2 (Fig. 6), Δ_b, and θ (Fig. 2). (Glutamate C-2, dashed lines; glutamate C-3, C-4, solid lines.) The signal intensities are calculated for J of glutamate C-2 = 150 Hz and J of glutamate C-3, 4 = 130 Hz.

C-2, between which the chemical shift difference is only about 0.5 ppm, are clearly separated (Fig. 10). The stacked plots shows amino acid metabolism in the brain in that the glutamate C-4 appears immediately after the administration of glucose, followed by the appearance of glutamate C-2, C-3 and glutamine C-2, C-3, C-4 (Fig. 11).

DISCUSSION

In vivo ^{13}C spectroscopy requires sensitivity, localization, and metabolite peak separation. Since the proposed polarization transfer methods are ^{13}C detection methods, they show good metabolite peak separation. The other items, sensitivity and localization, are discussed, and LINEPT is compared with LODEPT in sensitivity.

Sensitivity

LINEPT and LODEPT include many RF pulses, and inhomogeneity of the B_1 field causes signal loss. Thus, the surface coil used as the transmitter and receiver in the monkey experiments was not the most suitable for these polarization transfer methods. The best RF coil configuration is a transmitter volume coil with homogeneous B_1 field and a receiver surface coil with high sensitivity.

Localization

In LINEPT and LODEPT, the proton TE can be set to a value greater than $1/(2J)$ in LINEPT and greater than $1/J$ in LODEPT. Although the proton TE should not be set to a long value because of signal loss due to relaxation, the proton pulses can be optimized to obtain a good localization profile.

Comparison of LINEPT and LODEPT

One of the important brain metabolites in ^{13}C MRS using glucose is glutamate. Glucose C-1 is incorporated into glutamate C-2 (CH) and glutamate C-3, C-4 (CH_2). The maximum signal intensity conditions of the time intervals and RF flip angle, such as Δ_1, Δ_2 (Fig. 6), Δ_b, and θ (Fig. 2), are all the same as those in conventional INEPT and DEPT. These conditions differ between ^{13}C in CH and ^{13}C in CH_2. In decoupled LINEPT, the signal intensities of ^{13}C in CH and of ^{13}C in CH_2 are as follows:

$$\text{CH} \qquad S = \sin(2\pi J\Delta_1)\sin(\pi J\Delta_2) \qquad [4]$$

$$\text{CH}_2 \qquad S = \sin(2\pi J\Delta_1)\sin(2\pi J\Delta_2). \qquad [5]$$

In decoupled LODEPT, the signal intensities of ^{13}C in CH and of ^{13}C in CH_2 carbons are as follows:

$$\text{CH} \qquad S = \sin(\pi J\Delta_b)\sin(\theta) \qquad [6]$$

$$\text{CH}_2 \qquad S = \sin(\pi J\Delta_b)\sin(2\theta). \qquad [7]$$

The conditions under which the signal intensity of ^{13}C in CH and that of ^{13}C in CH_2 are equally high is the most suitable. These are when Δ_1 is 1.8 ms, Δ_2 is 2.43 ms, Δ is 3.6 ms, and θ is 60 degrees (Fig. 12). In decoupled LINEPT, the normalized signal intensities of glutamate C-2, C-3, and C-4 are 0.9 under these conditions. In decoupled LODEPT, these are 0.86. As a result, the decoupled LINEPT gives a slightly higher signal intensity than decoupled LODEPT. Since the proton TE can be set to a shorter value in decoupled LINEPT than in decoupled LODEPT, signal loss in the proton TE due to relaxation is also smaller in decoupled LINEPT than in decoupled LODEPT. Decoupled LINEPT is, therefore, more suitable for *in vivo* ^{13}C MRS in the brain.

CONCLUSIONS

LINEPT and LODEPT are three-dimensional localization ^{13}C spectroscopy methods with the following three features: good sensitivity, good metabolite separation, and good localization. The combination of a transmitter volume coil and a receiver surface coil is the best RF coil configuration to exploit these features. These features make these proposed methods powerful tools for the *in vivo* study of metabolism.

APPENDIX

The phase cycling scheme is obtained by product operator formalism using raising and lowering operators. INEPT is described using the arbitrary flip angles $b1$, $b2$, $b3$, $b4$, and b5 as shown below:

$$^1\text{H} \qquad b1\text{---}b2\text{---}b3$$

$$^{13}\text{C} \qquad\qquad b4\text{---}b5\text{-(Acquire)}.$$

The observable terms after the b5 pulse are as follows, neglecting proton chemical shifts. Enhanced terms obtained through polarization transfer:

$$\frac{i}{\sqrt{2}}(I_0S^+ + I_0S^-)\cos(b2)\sin(b1)\sin(b3)\sin(b5) \qquad [8]$$

$$\frac{i}{\sqrt{2}}(I_0S^+ + I_0S^-)\cos(b4)\sin(b1)\sin(b3)\sin(b5) \qquad [9]$$

$$i\cdot(I_0S^+ + I_0S^-)\cos(b5)\sin(b1)\sin(b3)\sin(b4) \qquad [10]$$

$$i\cdot(I_0S^+ + I_0S^-)\cos(b1)\sin(b2)\sin(b3)\sin(b5). \qquad [11]$$

Unenhanced terms obtained using only ^{13}C pulses:

$$(I_0S^+ + I_0S^-)\cos(b3)\sin(b4) \qquad [12]$$

$$-\frac{i}{2}(I_0S^+ + I_0S^-)\cos(b5)\sin(b4) \qquad [13]$$

$$-\frac{i}{\sqrt{2}}(S^+ + S^-)\cos(b4)\sin(b5). \qquad [14]$$

Under the INEPT condition, where $b1$, $b3$, and $b5$ equal 90 degrees and $b2$ and $b4$ equal 180 degrees, only Eqs. [8] and [9] are nonzero; note that Eqs. [8] and [9] are polarization transfer terms and the phase cycling scheme is designed to eliminate the other terms. Since the plus and minus signs of only the sine terms are inverted when the phase of RF pulse is inverted, attention should be paid to the sine terms in observable terms when designing the scheme. The sine terms in Eqs. [8] to [14] are highlighted below:

	$b1$	$b2$	$b3$	$b4$	$b5$
Eq. [8]	sine		sine		sine
Eq. [9]	sine		sine		sine
Eq. [10]	sine		sine	sine	
Eq. [11]		sine	sine		sine
Eq. [12]				sine	
Eq. [13]				sine	
Eq. [14]					sine

For example, Eqs. [8], [9], [10], and [11] can be separated from Eqs. [12], [13], and [14] by $b3$ phase cycling. This allows four-phase cycling schemes for obtaining only Eqs. [8] and [9] to be designed as follows:

Phase-cycling-1: $b1$-phase $(x, -x, x, -x)$, $b4$-phase $(x, x, -x, -x)$ and receiver phase $(x, -x, x, -x)$.

Phase-cycling-2: $b1$-phase $(x, x, -x, -x)$, $b5$-phase $(x, -x, x, -x)$, and receiver phase $(x, -x, -x, x)$.

ACKNOWLEDGMENTS

This work was performed as a part of the National Research & Development Programs for Medical and Welfare Apparatus under entrustment by the New Energy and Industrial Technology Development Organization (NEDO). The authors thank M. Oda, K. Hayashida, and H. Takahara (Institute of Life Science, Soka University) for their help in performing the animal experiments.

REFERENCES

1. W. P. Aue, S. Müller, and J. Seelig, Localized ^{13}C NMR spectra with enhanced sensitivity obtained by volume-selective excitation, *J. Magn. Reson.* **61,** 392–395 (1985).
2. D. G. Norris, N. Schuff, and D. Leibfritz, INEPT-enhanced ^{13}C spectroscopy using double-tuned surface coils, *J. Magn. Reson.* **78,** 362–366 (1988).
3. H. N. Yeung and S. D. Swanson, Imaging and localized spectroscopy of ^{13}C by polarization transfer, *J. Magn. Reson.* **83,** 183–189 (1989).
4. M. Saner, G. Mckinnon, M. Scheidegger, and P. Boesiger, Volume-

selective carbon-13 spectroscopy by localized polarization transfer, Proceedings of the Society of Magnetic Resonance in Medicine, 9th Annual Meeting, p. 1068, 1990.

5. G. A. Morris and R. Freeman, Enhancement of nuclear magnetic resonance signals by polarization transfer, *J. Am. Chem. Soc.* **101,** 760–762 (1979).

6. D. M. Doddrell, D. T. Pegg, and M. R. Bendall, Distortionless enhancement of NMR signals by polarization transfer, *J. Magn. Reson.* **48,** 323–327 (1982).

7. H. Watanabe, M. Yoshikawa, Y. Ishihara, K. Okamoto, Y. Suzuki, M. Oda, K. Oshio, T. Kanamatsu, and Y. Tsukada, 3-D localized ^{13}C spectroscopy by modified INEPT and DEPT, Proceedings of the Society of Magnetic Resonance, 3rd Annual Meeting, p. 1935, 1995.

8. K. L. Behar, O. A. C. Petroff, J. W. Prichard, J. A. Alger, and R. G. Shulman, Detection of metabolites in rabbit brain by ^{13}C NMR spectroscopy following administration of [1-^{13}C]glucose, *Magn. Reson. Med.* **3,** 911–920 (1986).